Exact solution for the singlet density distributions and second-order correlations of normal-mode coordinates for hard rods in one dimension

C. Daniel Barnes and David A. Kofke

Citation: The Journal of Chemical Physics **110**, 11390 (1999); doi: 10.1063/1.479080
View online: http://dx.doi.org/10.1063/1.479080
View Table of Contents: http://scitation.aip.org/content/aip/journal/jcp/110/23?ver=pdfcov
Published by the AIP Publishing

Exact solution for the singlet density distributions and second-order correlations of normal-mode coordinates for hard rods in one dimension

C. Daniel Barnes and David A. Kofke
Department of Chemical Engineering, State University of New York at Buffalo, Buffalo, New York 14260-4200

(Received 8 December 1998; accepted 25 March 1999)

We examine the distribution of normal-mode coordinates (defined via the eigenvectors of a chain of harmonic oscillators) for a system of purely repulsive hard rods in one dimension. We obtain an exact solution for the singlet density distribution, and separately for the covariances of the normal-mode coordinates. The hard-rod behavior is examined in terms of its deviation from the corresponding distributions for the system of harmonic oscillators. All off-diagonal covariances are zero in the hard-rod system, and the (on-diagonal) variances vary with the normal-mode wave number exactly as in the harmonic system. The detailed singlet normal-mode density distributions are very smooth but nonanalytic, and they differ from the (Gaussian) distributions of the corresponding harmonic system. However, all of the normal-mode coordinate distributions differ in roughly the same way when properly scaled by the distribution variance, and the differences vanish as $1/N$ in the thermodynamic limit of an infinite number of particles N. © *1999 American Institute of Physics.* [S0021-9606(99)51523-7]

I. INTRODUCTION

The system of hard rods in one dimension, also known as the Tonks gas,[1] is of interest as a prototype for studying the effect of steric exclusion on the behavior of fluids. The model exhibits no nontrivial behaviors—like all systems in one dimension, it does not undergo any phase transition—but many aspects of its behavior can be solved in closed form, and these solutions have provided some insight on the behavior of its higher-dimensional counterparts.[2] Usually the solutions do not invoke the thermodynamic limit to yield a result, so it is possible to examine the hard-rod model to gain some understanding of finite-size effects. Tonks was among the earliest to present formulas for the basic properties such as the equation of state[1] but, as pointed out by Robledo and Rowlinson,[3] the earliest solution was presented by Rayleigh.[4] It is now widely known that the van der Waals equation of state is exact in one dimension, in the sense that the van der Waals contribution to the pressure due to repulsion is exactly that of the hard-rod system.[1,5] Other properties known analytically for the hard-rod model include the pair and higher-order correlation functions for the pure system,[6] and mixtures,[7,8,17] the behavior in confined spaces,[3,9–11] and in the presence of other external fields,[12] and various dynamical properties.[13] Most recently, Corti and Debenedetti[14] as part of their studies of thermodynamic metastability turned to the hard-rod model for insight on the nature of voids (regions of space with no particles present) that arise as part of the natural fluctuations in fluid systems.

One of our research interests lies in the development of methods for computing free energies of solids by molecular simulation. One of the avenues that we have explored involves the use of a harmonic reference system, in which all interactions between the particles in the system take the form of simple harmonic springs. As is well known, the properties of this system can be solved analytically by diagonalizing the quadratic form of the internal energy, which effectively converts the system into a collection of independent harmonic oscillators. This is the basis of lattice dynamics.[15] Knowledge of the distribution of lattice vibration frequencies for a harmonic system is sufficient to determine the free energy and thus most other thermodynamic properties of interest, so the focus of study in lattice dynamics calculations and measurements is this quantity.

The usual approach taken in applying lattice dynamics calculations to estimate the properties of realistic systems involves an expansion of the intermolecular potential in powers of the molecular separations. Crystal symmetry causes the first-order terms to vanish, leaving the harmonic system as a natural reference. Corrections are then applied by considering higher-order terms in the expansion. This is not a viable route to the study of hard potentials (such as hard rods), because these potentials are not analytic. We deal instead with an approach that is couched more in the language of fluid-state theory. We are concerned with the singlet, pair, and higher-order correlations of the ''normal-mode coordinates'' occupied by the phonons. For the harmonic system, the singlet distribution is simply a Gaussian, and there are no higher-order correlations between the other modes. To the extent that these distributions are similar in a harmonic system and a system of interest, we have a viable means for estimating the target system's properties via molecular simulation. We reserve the details of this method for a separate publication. Instead we present here our exact solution for the singlet normal-mode coordinate distribution for the hard-rod model system.

The harmonic and hard-rod systems are very much unlike one another, and in fact they lie at the extreme limits of the Toda lattice,[1] which is an integrable one-dimensional

model that has been very helpful in understanding nonlinear lattice dynamics. We do not pursue the more general Toda lattice in our work because our ultimate aim is to apply the insights from the present study to develop molecular simulation methods for three-dimensional systems. The harmonic system retains its simplicity when extended this way, but the Toda lattice does not.

We begin in Sec. II by reviewing the treatment of harmonic systems, doing this mainly to establish the notation we use in subsequent sections. Then in Sec. III we review the hard-rod model and the solution for its partition function, and we consider a way to obtain simple statistical measures of the normal-mode correlations in the hard-rod system. Then in Sec. IV we present the analytic solution for the normal-mode singlet distribution, discuss the results in Sec. V, and provide concluding remarks in Sec. VI.

II. DESCRIPTION OF A SYSTEM OF HARMONIC OSCILLATORS

We consider a system of N harmonic oscillators in one dimension with only nearest-neighbor interactions. A configuration is described by the vector of coordinates $x^T=\{x_1,x_2,\ldots,x_N\}$, where x_k is the coordinate of the kth oscillator (x^T is the transpose of vector x). The energy for a given configuration is

$$U=U_0+W\sum_{k=1}^{N+1}(x_k-x_{k-1})^2. \tag{1}$$

Here we identify W as the strength of the harmonic interaction, which is the same for all pairs. Also, we bound the system by fixed walls, which for notational simplicity we assign coordinates $x_0=0$ and $x_{N+1}=L$. It is much more convenient to work with the coordinates that describe the deviation of each oscillator from its mean (or minimum-energy) position $x_k^0=kL/(N+1)$: $\gamma_k=x_k-x_k^0$. This step introduces new constant terms that can be lumped with U_0, but since all these contributions are not important to the present development we will drop them entirely. Then the energy may be written

$$U=\boldsymbol{\gamma}^T\mathbf{H}\boldsymbol{\gamma}, \tag{2}$$

where $\boldsymbol{\gamma}$ is the vector of deviation coordinates and $\mathbf{H}$ is an $N\times N$ tridiagonal matrix with diagonal elements equal to $+2W$ and secondary diagonal elements equal to $-W$.

Diagonalization of the above quadratic form results in an expression for the energy in terms of the N ''normal-mode'' coordinates that we designate $\eta^T=\{\eta_1,\eta_2,\ldots,\eta_N\}$, thus

$$U=\boldsymbol{\eta}^T\boldsymbol{\Lambda}\boldsymbol{\eta}, \tag{3}$$

where Λ is a diagonal matrix of eigenvalues of $\mathbf{H}$, and the simplicity of the original quadratic form permits their direct determination,

$$\lambda_m=2W\left(1-\cos\frac{m\pi}{N+1}\right), \tag{4}$$

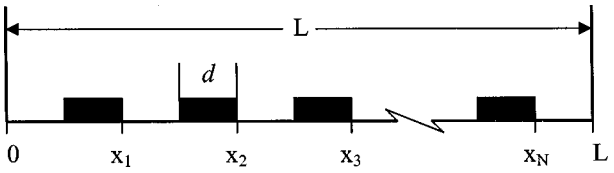

FIG. 1. System of N hard rods of equal length d and total system length L. The system is bounded by walls of infinite potential at 0 and L.

where λ_m is the mth diagonal element of Λ. The normal-mode coordinates η are simple linear transformations from the real-space deviations γ and are obtained from the eigenvectors of $\mathbf{H}$,

$$\boldsymbol{\eta}=\boldsymbol{\Phi}^{-1}\boldsymbol{\gamma}, \tag{5}$$

where Φ is the matrix with columns given by the eigenvectors of $\mathbf{H}$ and, because $\mathbf{H}$ is symmetric $\Phi^{-1}=\Phi^T$; also Φ is symmetric with elements

$$\phi_{mk}=\left(\frac{2}{N+1}\right)^{1/2}\sin\left(\frac{km\pi}{N+1}\right), \tag{6}$$

so $\Phi^{-1}=\Phi$.

The normal-mode singlet density distribution $p_m(\eta_m)$ describes the distribution of values adopted by the normal-mode coordinate η_m. Formally it may be expressed as an ensemble average

$$p_m(\eta)=\langle\delta(\eta_m-\eta)\rangle, \tag{7}$$

where δ is the Dirac delta function. For the simple system of harmonic oscillators, this distribution function is a Gaussian with zero mean

$$p_m^{\mathrm{harm}}(\eta)=(\pi/\lambda_m)^{-1/2}\exp(-\lambda_m\eta^2), \tag{8}$$

so the variance in the distribution of the coordinate η_m is given directly by its eigenvalue $\langle\eta_m^2\rangle=(2\lambda_m)^{-1}$; the normal-mode coordinates for the harmonic system are uncorrelated, i.e., $\langle\eta_m\eta_l\rangle=0$, $m\neq l$, which is why they are designated ''normal modes.''

III. HARD-ROD MODEL AND SECOND-ORDER CORRELATIONS

We consider a system of N hard rods of equal length σ, bounded by hard walls (of infinite potential) separated by a distance L as pictured Fig. 1.

We could just as easily have worked within periodic boundaries. Note that the coordinate x_k specifies the position of the right-hand side of the rod. The configuration integral for the hard-rod system is given by

$$Q_{\mathrm{HR}}=\frac{1}{N!}\int_0^L dx_N\int_0^L dx_{N-1}\cdots\int_0^L dx_2\int_0^L dx_1\exp(-\beta U_{\mathrm{HR}}), \tag{9}$$

where U_{HR} is the energy of the system, which is infinite if there is any overlap (including overlaps with the walls) and zero otherwise.

The usual route to solving the partition function involves ordering the rods as suggested by Fig. 1, so that $x_k > x_j$ for $k > j$. This eliminates the degeneracy factor $N!$ and changes the limits of integration for each rod,

$$Q_{\mathrm{HR}} = \int_{N\sigma}^{L} dx_N \int_{(N-1)\sigma}^{x_N-\sigma} dx_{N-1} \cdots \int_{2\sigma}^{x_3-\sigma} dx_2 \int_{\sigma}^{x_2-\sigma} dx_1 . \tag{10}$$

The Boltzmann weighting can be removed because the limits of integration preclude any overlap. A change of coordinates is now applied

$$y_k = x_k - k\sigma, \tag{11}$$

so the partition function becomes

$$Q_{\mathrm{HR}} = \int_0^{L-\sigma N} dy_N \int_0^{y_N} dy_{N-1} \cdots \int_0^{y_3} dy_2 \int_0^{y_2} dy_1 . \tag{12}$$

The nested integrals are now easily evaluated, yielding

$$Q_{\mathrm{HR}} = \frac{(L-\sigma N)^N}{N!}. \tag{13}$$

Various statistics about the hard-rod positions and correlations are of interest. It is easier to derive them in terms of the convenience coordinates y defined in Eq. (11) and then transform the averages to the real coordinates x. The average y value adopted by the kth rod is

$$\begin{aligned} \langle y_k \rangle &= \frac{1}{Q_{\mathrm{HR}}} \int_0^{L-\sigma N} dy_N \int_0^{y_N} dy_{N-1} \cdots \\ &\quad \times \int_0^{y_{k+1}} dy_k y_k \cdots \int_0^{y_3} dy_2 \int_0^{y_2} dy_1 \\ &= \frac{k}{N+1}(L-\sigma N), \end{aligned} \tag{14}$$

so the average x coordinate is

$$\begin{aligned} \langle x_k \rangle &= \langle y_k \rangle + k\sigma \\ &= \frac{k}{N+1}(L+\sigma). \end{aligned} \tag{15}$$

which, as one might expect, is roughly the corresponding fractional distance to the end of the system's length.

Again it is convenient to assign each rod a ''lattice-site'' coordinate and focus on the statistics associated with deviations from this position. We do this even though the hard-rod system does not form a true crystalline phase. As with the harmonic system above, we define the lattice site for rod k as its average position, and introduce the deviation coordinates $\gamma_k \equiv x_k - \langle x_k \rangle$; obviously $\langle \gamma_k \rangle = 0$.

Likewise, the average pair correlate is given from the two-body average

$$\begin{aligned} \langle y_j y_k \rangle &= \frac{1}{Q_{\mathrm{HR}}} \int_0^{L-\sigma N} dy_N \int_0^{y_N} dy_{N-1} \cdots \\ &\quad \times \int_0^{y_{k+1}} dy_k y_k \cdots \int_0^{y_{j+1}} dy_j y_j \cdots \int_0^{y_3} dy_2 \int_0^{y_2} dy_1 \\ &= \frac{j(k+1)}{(N+1)(N+2)}(L-\sigma N)^2, \quad k \geqslant j. \end{aligned} \tag{16}$$

Then

$$\begin{aligned} \langle \gamma_j \gamma_k \rangle &= \langle x_j x_k \rangle - \langle x_j \rangle \langle x_k \rangle \\ &= \langle y_j y_k \rangle - \langle y_j \rangle \langle y_k \rangle \\ &= \left(\frac{L-\sigma N}{N+1} \right)^2 \frac{j(N+1-k)}{N+2}, \quad k \geqslant j. \end{aligned} \tag{17}$$

We now make our first connection between the hard-rod model and the harmonic system reviewed in Sec. II. We consider the normal-mode coordinates introduced in Sec. II, but we examine statistics for them when ensemble averaged over the hard-rod configurations. The normal-mode deviation coordinates are still defined in terms of the real-space deviation coordinates as in Eq. (5), and it is clear that the mean value of the normal-mode coordinate $\langle \eta_m \rangle$ is still zero for all m. We turn then directly to second-moment averages of these coordinates. These may be obtained from the results just presented for $\langle \gamma_j \gamma_k \rangle$ via the transformation

$$\langle \boldsymbol{\eta} \boldsymbol{\eta}^T \rangle = \boldsymbol{\Phi} \langle \boldsymbol{\gamma} \boldsymbol{\gamma}^T \rangle \boldsymbol{\Phi} \tag{18}$$

(in writing the result this way we have applied some of the simplifying features of $\boldsymbol{\Phi}$). Inserting the result for $\langle \gamma_j \gamma_k \rangle$ and Eq. (6) for $\boldsymbol{\Phi}$, after some manipulation the (co)variance of the normal-mode deviations is given by

$$\begin{aligned} \langle \eta_m \eta_n \rangle &= \frac{1}{(N+2)\left(1-\cos\dfrac{m\pi}{N+1}\right)} \left[\frac{L-\sigma N}{N+1} \right]^2 \\ &\quad \times \sum_{j=1}^{N} \sin\frac{jm\pi}{N+1} \sin\frac{jn\pi}{N+1}. \end{aligned} \tag{19}$$

The very surprising result of this analysis is that all the second-order statistics for the distributions of the normal-mode coordinates are the same in the hard-rod system as in the harmonic oscillators for which the coordinates are derived. For $m \neq n$ in Eq. (19), the sine functions are orthogonal so the summation is zero, and therefore the covariance is zero. For $m = n$, the sine functions are of course equivalent and the variance is given by

$$\langle \eta_m^2 \rangle = \frac{(N+1)}{2(N+2)\left(1-\cos\dfrac{m\pi}{N+1}\right)} \left[\frac{L-\sigma N}{N+1} \right]^2 . \tag{20}$$

Interestingly, these statistics and those from the harmonic system differ by the same multiplicative constant $(L-\sigma N)^2/(N+2)(N+1)$ for all m, which means the hard-rod averages could all be made equal to their harmonic counterparts by appropriate selection of the harmonic spring constant W.

IV. NORMAL-MODE SINGLET DISTRIBUTIONS

We now turn to an analysis of the detailed distributions of the normal-mode coordinates averaged over configurations of the hard-rod system. Here differences between the hard-rod and harmonic systems begin to emerge.

We start with the description of $p_m(\eta)$ as the ensemble-averaged delta function given by

$$p_m(\eta)=\frac{1}{Q_{\mathrm{HR}}}\int_0^{L-\sigma N}dy_N\int_0^{y_N}dy_{N-1}\cdots \times\int_0^{y_3}dy_2\int_0^{y_2}dy_1\,\delta(\eta-\eta_m(\mathbf{y})). \tag{21}$$

We will introduce the linear transformation that gives the normal-mode coordinate in terms of the hard-rod convenience coordinates $\mathbf{y}$,

$$\eta_m(\mathbf{y})=\sum_{k=1}^{N}\phi_{mk}\gamma_k(y_k) =\sum_{k=1}^{N}\phi_{mk}\left(y_k-\frac{k}{N+1}Y\right), \tag{22}$$

where we have defined

$$Y=L-\sigma N. \tag{23}$$

A key step in the development is writing the delta function in its Fourier transform representation

$$\delta(x)=\int_{-\infty}^{\infty}e^{itx}\,dt,$$

where $i=\sqrt{-1}$. With these transformations the singlet normal-mode density distribution can be expressed

$$p_m(\eta)=\frac{1}{2\pi Q_{\mathrm{HR}}}\int_{-\infty}^{\infty}dt\exp[it(\eta+\eta_m^0)]\int_0^Y dy_N \times\exp[-it\phi_{mN}y_N]\cdots\int_0^{y_2}dy_1\exp[-it\phi_{m1}y_1], \tag{24}$$

where

$$\eta_m^0\equiv\frac{Y}{N+1}\sum_{k=1}^{N}\phi_{mk}k. \tag{25}$$

The task now is to develop a means to perform the nested integrals over the y coordinates. This can be accomplished by casting them in terms of a recursion relation:

$$Q_k^{(m)}(t,y)=\int_0^y dy_k\exp[-it\phi_{mk}y_k]\cdots\int_0^{y_2}dy_1 \times\exp[-it\phi_{m1}y_1] =\int_0^y dy_k\exp[-it\phi_{mk}y_k]Q_{k-1}^{(m)}(t,y_k), \tag{26}$$

so

$$p_m(\eta)=\frac{1}{2\pi}\frac{1}{Q_{\mathrm{HR}}}\int_{-\infty}^{\infty}dt\exp[it(\eta+\eta_m^0)]Q_N^{(m)}(t,Y) =\frac{1}{Q_{\mathrm{HR}}}\hat{Q}_N^{(m)}(\eta+\eta_m^0,Y), \tag{27}$$

where the caret indicates a Fourier transform of the first argument of $Q_N^{(m)}$. The recursion relation forms a convolution that yields to application of the Laplace transform (of the second argument of $Q_N^{(m)}$; the Laplace transform is indicated by a tilde):

$$L[Q_k^{(m)}(t,y)]\equiv\tilde{Q}_k^{(m)}(t,s) =\frac{1}{s}\tilde{Q}_{k-1}^{(m)}(t,s+it\phi_{mk}). \tag{28}$$

Repeated application of this formula with an obvious termination condition at $k=1$ produces

$$\tilde{Q}_N^{(m)}(t,s)=\prod_{k=1}^{N+1}(s+itA_k^{(m)})^{-1}, \tag{29}$$

where

$$A_k^{(m)}\equiv\sum_{j=k}^{N}\phi_{mj} =\left(\frac{2}{N+1}\right)^{1/2} \times\frac{\sin\left[\frac{m\pi(k+N)}{2(N+1)}\right]\sin\left[\frac{m\pi(N+1-k)}{2(N+1)}\right]}{\sin\left[\frac{m\pi}{2(N+1)}\right]}, \tag{30}$$

where the latter equality is obtained as a trigonometric identity.

Before performing the inverse transform it is important to note that terms inside the product may be degenerate. We let $\overline{A}_k^{(m)}$, $k=1\cdots\overline{N}\leqslant N+1$ be the unique values of $A^{(m)}$ and we indicate their degeneracy in $A^{(m)}$ by ω_k; Eq. (29) can be rewritten as:

$$\tilde{Q}_N^{(m)}(t,s)=\prod_{k=1}^{\overline{N}}(s+it\overline{A}_k^{(m)})^{-\omega_k}. \tag{31}$$

The general solution for the inverse Laplace transform of Eq. (31) is[16]

$$Q_N^{(m)}(t,Y)=L^{-1}[\tilde{Q}_N^{(m)}(t,s)] =\sum_{k=1}^{\overline{N}}\sum_{j=1}^{\omega_k}\frac{C_{k,j}^{(m)}Y^{(\omega_k-j)}}{(\omega_k-j)!(j-1)!}\frac{e^{-itY\overline{A}_k^{(m)}}}{(it)^{N+j-\omega_k}}, \tag{32}$$

where

$$C_{k,j}^{(m)}=\lim_{s\to-\overline{A}_k^{(m)}}\left(\frac{d^{(j-1)}}{ds^{(j-1)}}\prod_{l\neq k}^{\overline{N}}(s+\overline{A}_l^{(m)})^{-\omega_l}\right). \tag{33}$$

These coefficients for $j=1$ are not particularly difficult,

$$C_{k,l}^{(m)}=\prod_{\substack{l=1\\ l\neq k}}^{\overline{N}}(\overline{A_l^{(m)}}-\overline{A_k^{(m)}})^{-\omega_l}. \tag{34}$$

Otherwise the $C_{k,j}^{(m)}$ coefficients can be treated via a recursion relation, but the computer code that results is not very efficient. In general, great variation in the degeneracy may be observed from one term to the next and it is difficult to identify a pattern in this behavior that might be used to speed up the calculation. However, the form of the degeneracy is particularly simple if we restrict N such that $N+1$ is prime. We demonstrate in the Appendix that in this situation all of the elements of $A^{(m)}$ are nondegenerate when m is odd, and all elements but one are doubly degenerate when m is even. In particular,

$$\overline{A_k^{(m)}}=A_k^{(m)}, \quad k=1\cdots\overline{N}=(N+1) \quad (m \text{ odd}),$$

and

$$\overline{A_k^{(m)}}=A_k^{(m)}=A_{N+2-k}^{(m)},$$
$$k=1\cdots(\overline{N}-1)=(N/2) \quad (m \text{ even}),$$
$$\overline{A_k^{(m)}}=A_k^{(m)}, \quad k=\overline{N}=(N/2)+1.$$

In practice restricting N this way barely reduces the generality of the development, so we proceed from here using this simplification.

Then for m even the $j=2$ coefficients are needed in addition to those for $j=1$, and Eq. (34) becomes

$$C_{k,2}^{(m)}=-C_{k,1}^{(m)}\left[(A_N^{(m)}-A_k^{(m)})^{-1}+2\sum_{\substack{l=1,\\ l\neq k}}^{N/2+1}(A_l^{(m)}-A_k^{(m)})^{-1}\right] \quad (m \text{ even}), \tag{35}$$

while for m odd, only $j=1$ is needed, and the inverse transform may be written directly

$$Q_N^{(m)}(t,Y)=(it)^{-N}\sum_{k=1}^{N}C_{k,1}^{(m)}e^{-itYA_k^{(m)}} \quad (m \text{ odd}). \tag{36}$$

The singlet density distribution is finally recovered by performing the Fourier integration with respect to t as indicated in Eq. (27). The terms in $Q_N^{(m)}(t,Y)$ are of the form $t^{-m}\exp(ibt)$, for which the Fourier transform from t to η is

$$\frac{(\eta+b)^{n-1}}{(n-1)}\left(-\frac{1}{2}+\Theta(\eta+b)\right), \tag{37}$$

where Θ is the Heaviside function.

Thus the singlet distribution is a sum of polynomials in η, each with its own Heaviside function that ''switches on'' at a particular $\eta=-b$, where b is in general different for each term of the sum. The net effect of the Heaviside function (when added to $-1/2$) is to change the sign of the coefficient of the corresponding term in the sum. For η large and negative, all Heaviside functions are ''off,'' and we have a simple sum of polynomials; for η large and positive we have the same polynomial sum but with the opposite sign. Clearly the probability density must be zero for sufficiently large positive or large negative values of η, so we must conclude that this polynomial sum is identically zero. We have not attempted to otherwise demonstrate this result analytically, but we do find it to be true empirically. A consequence is that we may drop the $-1/2$ from Eq. (37). Upon taking this step we put together all the foregoing developments to arrive at our final working expression for $p_m(\eta)$,

$$p_m(\eta)=\frac{1}{Q_{\mathrm{HR}}}\frac{1}{(N-1)}\sum_{k=1}^{N+1}C_{k,1}^{(m)}(\eta+\eta_m^0-YA_k^{(m)})^{N-1}\times\Theta(\eta+\eta_m^0-YA_k^{(m)}) \quad (m \text{ odd}), \tag{38}$$

$$p_m(\eta)=\frac{1}{Q_{\mathrm{HR}}}\times\left(\sum_{k=1}^{N/2}\left(\left(\frac{C_{k,1}^{(m)}}{(N-2)!}+\frac{C_{k,2}^{(m)}}{(N-1)!}(\eta+\eta_m^0-YA_k^{(m)})\right)(\eta+\eta_m^0-YA_k^{(m)})^{N-2}\Theta(\eta+\eta_m^0-YA_k^{(m)})\right.\right.$$
$$\left.\left.-\frac{(\eta+\eta_m^0-YA_{N/2+1}^{(m)})^{N-1}}{(N-1)!}C_{N/2+1,1}^{(m)}\Theta(\eta+\eta_m^0-YA_{N/2+1}^{(m)})\right) \quad (m \text{ even}). \tag{39}$$

Again, this result applies for $N+1$ a prime number. In summary, the terms appearing in this equation are as follows: Q_{HR} is the hard-rod partition function given by Eq. (9); $C_{k,1}^{(m)}$ and $C_{k,2}^{(m)}$ are given by Eqs. (34) and (35), respectively, and are functions of the mode m and index k; η_m^0 is given by Eq. (25), Y is given by Eq. (23); $A_k^{(m)}$ is given by Eq. (30); Θ is the Heaviside function and is zero when its argument is less than zero and unity when its argument is greater or equal to zero; N is the number of hard rods, and so is also the number of modes.

V. DISCUSSION

Plots of the exact solution for the singlet density distribution for systems of $N=4$, 10, and 22 rods are presented in Figs. 2–4, respectively. Plots for larger values of N become

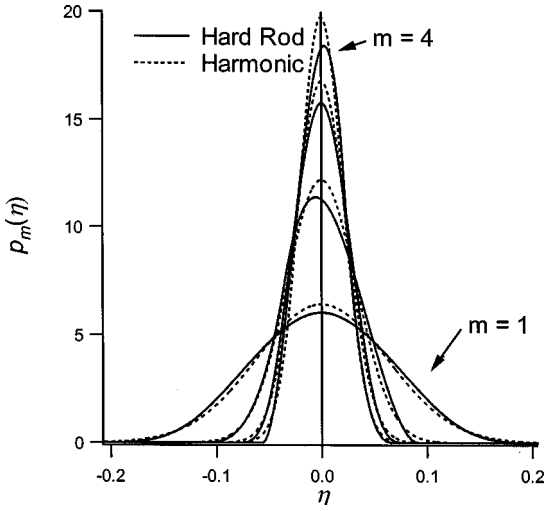

FIG. 2. Singlet normal-mode density distribution for a system of four hard rods of width $d=1$ at a density Nd/L of 0.95 shown with the corresponding harmonic distribution of the same variance. The four sets of curves correspond to each of the four normal modes, where $m=1$ is the lowest frequency mode (longest wavelength) and $m=4$ is the highest frequency mode.

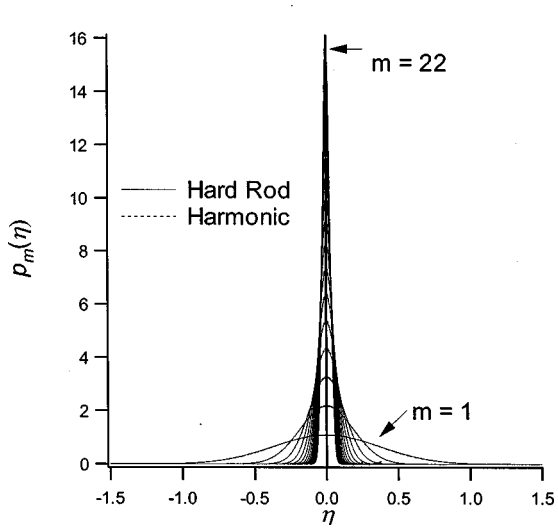

FIG. 4. Singlet normal-mode density, as presented in Fig. 2, but for $N=22$ particles. At this scale the hard rod and harmonic curves are virtually indistinguishable.

increasingly difficult to construct. The distribution function is given by a sum of Nth order polynomials, which tend to offset each other as η increases, eventually canceling exactly for η beyond its maximum value. As η approaches its maximum, roundoff errors in summing the polynomials cause difficulties in computing the density distribution. However, as discussed below, results up to $N=22$ are sufficient to uncover the trends in the behavior of the distribution function. In each plot curves are shown for several values of the mode number m; for $N=4$ the corresponding (Gaussian) distributions for a pure harmonic oscillator (with spring constant selected to result in the same variance) are presented in Figs. 2–4. The hard-rod distributions appear to be very smooth, even though at many points they are nonanalytic. The nonanalyticities come from terms of the form $(\eta-b_0)^{N-1}\Theta(\eta-b_0)$, so the distribution is nonanalytic at each point $\eta=b_0$ where a Heaviside function is turned on, but the discontinuity appears only in the $N-1$ derivative.

A careful look at the distributions for $N=4$ shows that the curves for m odd appear to be symmetric, while those for m even exhibit asymmetry. For larger N the asymmetries appear to be attenuated, and it becomes increasingly difficult to distinguish the hard-rod distributions from Gaussian forms. More about the symmetry of the distributions can be uncovered by examining their behavior at the two tails, just before they become zero as $|\eta|$ increases. On the left-hand side, $p(\eta)$ is given by the polynomial multiplying the first Heaviside function to be turned on, while on the right-hand side the distribution is given by the negative of the polynomial multiplying the last Heaviside function to be turned on (because turning this last term on exactly cancels the part before the distribution is zero). For m odd, the distribution just before it vanishes on the right-hand side is

$$p_m(\eta)=\frac{1}{(N-1)!Q_{\mathrm{HR}}}C_{\mathrm{min},1}(\eta+\eta_m^0-YA_{\mathrm{min}}^{(m)})^{(N-1)}, \tag{40}$$

while on the left-hand side

$$p_m(\eta)=\frac{1}{(N-1)!Q_{\mathrm{HR}}}C_{\mathrm{max},1}(\eta+\eta_m^0-YA_{\mathrm{max}}^{(m)})^{(N-1)}. \tag{41}$$

where ''max'' and ''min,'' respectively, refer to the values for k for the largest and smallest values of $A_k^{(m)}$. We find empirically $C_{\mathrm{min},1}=C_{\mathrm{max},1}$ and $(\eta_m^0-YA_{\mathrm{min}}^{(m)})=-(\eta_m^0-YA_{\mathrm{max}}^{(m)})$, indicating that the m-odd distributions are symmetric in terms of their vanishing points and their behavior approaching these points. For m even $A_k^{(m)}$ is the maximum A for $k=N/2+1$ if $m/2$ is odd, while this k gives the smallest A if $m/2$ is even. In either case, the distribution at the other end vanishes according to

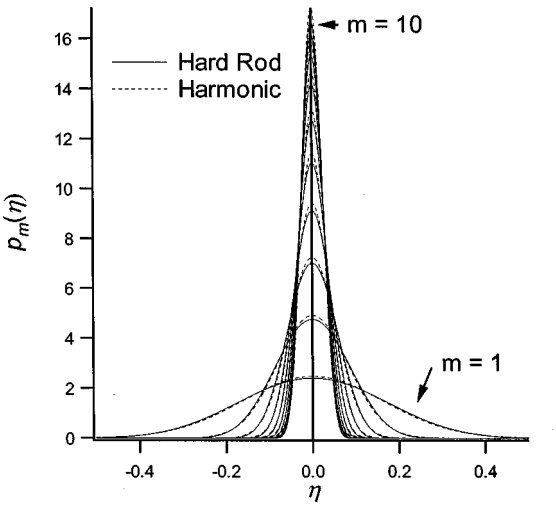

FIG. 3. Singlet normal-mode density, as presented in Fig. 2, but for $N=10$ particles.

$$p_m(\eta) = \frac{1}{(N-1)!\,Q_{\mathrm{HR}}}[C_{k,1}(\eta + \eta_m^0 - YA_k^{(m)})^{(N-2)} + C_{k,2}(\eta + \eta_m^0 - YA_k^{(m)})^{(N-1)}]. \quad (42)$$

The point is that the neither the vanishing point nor the functional form near the vanishing point is symmetric in this case. Based on this limited observation of the analytic form of the distributions, along with the observed shape of the complete distributions, we would judge the distributions for m odd to be completely symmetric about the origin, while those for m even are not.

We can speculate on the origins of this symmetry behavior. We note that the normal modes corresponding to m odd describe collective modes that are symmetric about the center of mass of the system, while the modes corresponding to m even describe motions that are antisymmetric about this point. Connected to this, and more important, is the number of nodes associated with each collective motion. The nodes are points where the deviation of the rods from their lattice sites changes sign. Thus each node represents a point at which the rods locally are being compressed or expanded. For m odd, the number of such nodes is *even*, meaning the number of compression points is the same regardless of the sign of η; for m even the number of nodes is *odd*, so the number of compression points depends on the sign of η. For a harmonic system, compression and expansion of the particles is the same in terms of the energy cost, but for hard rods there is obviously a severe energy asymmetry between the two motions.

The analysis of Sec. III indicates that the hard-rod normal mode distributions have variances (and covariances) identical to the harmonic system that defines the normal mode coordinates. This result suggests that comparison of the behavior of various modes for a given N can be facilitated by scaling all normal-mode coordinates by the corresponding variance exhibited in the harmonic system. If the hard-rod normal-mode singlet distributions were identical to those for a harmonic system, then this transformation would cause all the distributions to collapse onto a single Gaussian curve of unit variance. To highlight the difference from harmonic behavior, we examine in Figs. 5 and 6 the difference in these scaled distributions from the unit-variance Gaussian, for $N=4$ and 10, respectively. For given N, the scaled distributions for m odd are mutually identical. Although for $N=4$ the scaled curves for m even do not show a common behavior, as N grows these curves all approach the common distribution for m odd. As shown in Fig. 6, for N as small as 10 all the scaled distributions are virtually indistinguishable from one another.

Figures 5 and 6 also provide some indication of the size dependence of the scaled distributions. The maximum deviation is of the order of 0.6 for $N=4$, while for $N=10$ it has diminished to about 0.2. This observation suggests a simple N dependence of the scaled distribution. In Fig. 7 the variance-scaled distributions are multiplied by N, and the resulting curves are presented for several values of N from $N=4$ to $N=22$. There is a clear convergence to a universal behavior which seems to be almost reached at the largest

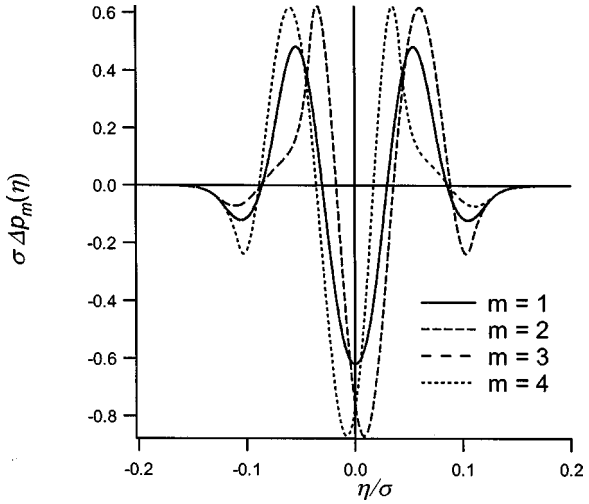

FIG. 5. Difference between the hard rod and harmonic and singlet normal mode density distributions for the system of four hard rods shown in Fig. 2. The axes are scaled by the variance of each distribution. The curves for $m=1$ and $m=3$ are indistinguishable.

value of N used to construct the plot. In the thermodynamic limit, all singlet normal-mode density distributions adopt Gaussian forms, with variances distributed exactly as in the harmonic system. Differences between the hard-rod configurations and those of the harmonic system must manifest themselves at the level of two-''body'' and higher correlations among the normal-mode coordinates. However, given that the normal-mode covariances are zero [Eq. (19)], cooperative behaviors at the pair level are not likely to show much, if any, deviation of the distributions from the harmonic forms.

Finally we consider the effect of density on the results. In Fig. 8 we present the limiting form of variance- and particle-number-scaled singlet-density deviation, as a function of the system density $N\sigma/L$. We observe the same qualitative behavior over all densities. As the density is in-

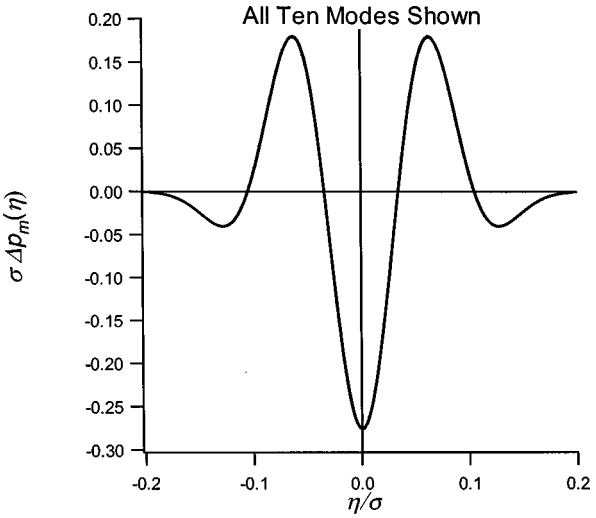

FIG. 6. As in Fig. 5, but for $N=10$. The differences between the odd and even modes which are very apparent in Fig. 5 (four hard rods) are now essentially indistinguishable.

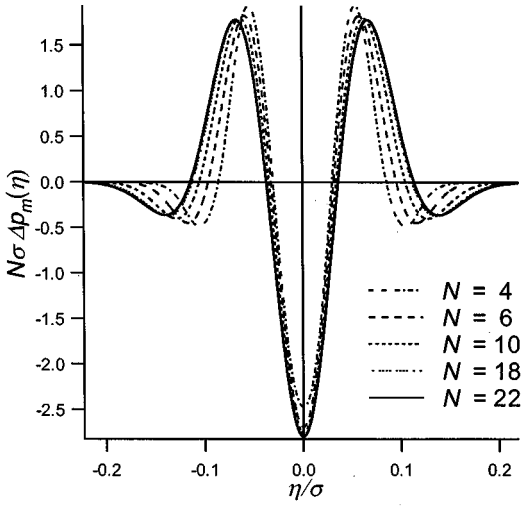

FIG. 7. Scaled difference between the hard rod and harmonic singlet normal-mode density distributions various system sizes. Difference are scaled by particle number as indicated. The systems converge to a limiting curve with increasing system size.

creased, the scaled deviation increases in magnitude reflecting the increasing importance of the repulsive interactions on the hard-rod behavior.

VI. CONCLUDING REMARKS

The hard-rod model represents a highly anharmonic system. The hard-rod potential cannot be expanded as a power series in the pair separation as is usually done to connect an anharmonic system to a harmonic reference. Yet the model exhibits at a basic level, behavior that conforms completely to that of a harmonic system: all of the singlet normal-mode density distributions are exactly harmonic in the thermodynamic limit, and all the second-order correlations follow harmonic behavior as well. Repulsion is an important feature of real intermolecular potentials, and is usually the largest source of anharmonicity. This work suggests that a viable route to modeling the behavior of real solids from a harmonic reference would consider perturbations in their normal-mode density distributions rather than in the intermolecular potential.

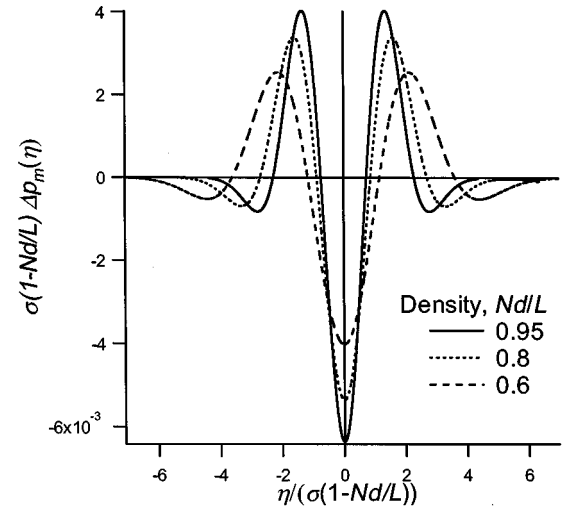

FIG. 8. Scaled difference between the hard rod and harmonic singlet normal-mode density distributions for $N=22$ at densities (Nd/L) of 0.95, 0.80, and 0.60. The curves are scaled by $\sigma(1-Nd/L)$ as shown.

APPENDIX

Here we show that for $N+1$ prime and m odd, the summations $A_k^{(m)}$ of the eigenvector coefficients $\phi_j^{(m)}$ for $j=k$ to $N+1$ are unique for all $k\exists 1\leqslant k\leqslant N+1$, while for m even, the summations are doubly degenerate for the same range of k except when $k=N/2+1$, for which the summation $A_{N/2+1}^{(m)}$ is unique.

Manipulations using trigonometric identities transform the expression for $A_k^{(m)}$ given in Eq. (30) into a form more useful for this analysis; in the end we have

$$A_k^{(m)}=\left(\frac{2}{N+1}\right)^{1/2}\frac{\cos[a]-\cos[a(2(N-k+1)+1)]}{2\sin[a]}, \tag{A1}$$

where $a=m\pi/2(N+1)$. The only k-dependent term in this expression is $\cos[a(2(N-k+1)+1)]$ so any uniqueness or degeneracy with respect to k derives from this term, and we need consider only it in the subsequent analysis.

Whenever the cosine functions are equal for different values of k, $A_{k_i}^{(m)}=A_{k_j}^{(m)}$, there is a degeneracy. There are two cases to check. First, if the arguments of the cosine differ by an integer multiple of 2π, their cosines will be equal. Second, cosine is a even function, so that $\cos[b]=\cos[-b+2\pi q]$ for q any integer including zero, and degeneracy may arise this way.

Consider the first case. There will be degeneracy for two values of k, $k_j\neq k_i$, if

$$a(2(N-k_i+1)+1)-a(2(N-k_j+1)+1)=2\pi q,$$
$$q=\ldots,-2,-1,1,2..., \tag{A2}$$

which simplifies to

$$k_j-k_i=(N+1)\frac{2q}{m}.$$

The difference in k's, k_j-k_i, must be an integer, so the right-hand side must also be an integer if there exist two values of k that satisfy this relation. If we choose $N+1$ prime, there is no rational number (less than unity) by which it can be multiplied that would result in an integer, so the quantity $2q/m$ must also be an integer. Since both q and m are integers, this requires that q be an integer multiple of m for m odd, or an integer multiple of $m/2$ for m even. In any case the smallest possible value for the right-hand side is $N+1$, but at the same time the largest possible magnitude for the difference in k's is $N+1-1=N$. Obviously the difference in k's cannot simultaneously be less than or equal to N *and* greater than or equal to $N+1$, so we conclude that there exists no pair of k values for which the respective arguments to the cosine differ by a multiple of 2π (for $N+1$ prime).

For the second case there will be degeneracy if

$$-a(2(N-k_j+1)+1)+2\pi q=a(2(N-k_i+1)+1), \qquad q=\ldots,-2,-1,0,1,2,..., \tag{A3}$$

which simplifies to

$$k_j+k_i=2\frac{N+1}{m}(m-q)+1. \tag{A4}$$

Since q can represent any integer, the term $(m-q)$ can take on any integral value, so we simply replace it by q, and the equation becomes

$$k_j+k_i=(N+1)\frac{2q}{m}+1. \tag{A5}$$

Again, choosing $N+1$ prime, and following the same arguments for the first case, q must be integer multiples of m for m odd, and integer multiples of $m/2$ for m even. Now we have a sum of two k's, the largest possible value being $N+1+N=2N+1$. For m odd the smallest possible value of the right-hand side occurs for $q=m$, which leaves $k_j+k_i=2N+3$, which exceeds the bound for the sum. Thus no pair of k's can lead to a degeneracy (m odd, $N+1$ prime). For m even, the smallest value of the right-hand side occurs for $q=m/2$. Then $k_j+k_i=N+2$, and we have an expression that can be satisfied by some pairs of k values; in particular these pairs are

$$\{(N+1,1),(N,2),(N-1,3),\ldots,(N/2+3,N/2-1) \times(N/2+2,N/2)\}.$$

Note that since $N+1$ is prime, N is even, so $N/2$ is an integer. From this set it can be seen that $A_{N+1}^{(m)}=A_1^{(m)}$, $A_N^{(m)}=A_2^{(m)}$, etc. For m even, all the terms are doubly degenerate with the single exception of the $N/2+1$ term, which is unique. There is no triple or higher degeneracy.

We have shown that by choosing $N+1$ prime, the summations of the eigenvector coefficients are unique for all k for m odd, and are doubly degenerate (symmetrically about $N/2+1$) for m even for all k with the exception of the $N/2+1$ term, for which the sum is unique.

[1] M. Toda, *Theory of Nonlinear Lattices*, 2nd ed. (Springer, Berlin, 1989), Vol. 20.
[2] E. H. Lieb and D. C. Mattis, *Mathematical Physics in One Dimension. Exactly Soluble Models of Interacting Particles* (Academic, New York, 1966).
[3] A. Robledo and J. S. Rowlinson, Mol. Phys. **58**, 711 (1986).
[4] L. Rayleigh, Nature (London) **45**, 80 (1891).
[5] M. Kac, E. Uhlenbeck, and P. C. Hemmer, J. Math. Phys. **4**, 216 (1963).
[6] Z. W. Salsburg, R. W. Zwanzig, and J. G. Kirkwood, J. Chem. Phys. **21**, 1098 (1953).
[7] J. Foidl, J. Chem. Phys. **85**, 410 (1986).
[8] E. Burgos and H. Bonadeo, J. Chem. Phys. **88**, 1163 (1988).
[9] P. A. Monson, Mol. Phys. **70**, 401 (1990).
[10] L. Tonks, Phys. Rev. **50**, 955 (1936).
[11] H. T. Davis, J. Chem. Phys. **93**, 4339 (1990).
[12] J. K. Percus, J. Stat. Phys. **15**, 505 (1976).
[13] D. W. Jepsen, J. Math. Phys. **6**, 405 (1965).
[14] D. S. Corti and P. G. Debenedetti, Phys. Rev. E **57**, 4211 (1998).
[15] M. Born and K. Huang, *Dynamical Theory of Crystal Lattices* (Clarendon, Oxford, 1954).
[16] M. Erdelyi and T. Oberhettinger, *Tables of Integral Transforms* (McGraw–Hill, New York, 1954), Vol. 1.
[17] T. K. Vanderlick, H. T. Davis, and J. K. Percus, J. Chem. Phys. **91**, 7136 (1989).